VIII International Conference on Fracture Mechanics of Concrete and Concrete Structures
FraMCoS-8
J.G.M. Van Mier, G. Ruiz, C. Andrade, R.C. Yu and X.X. Zhang (Eds)

ANCHORAGE STRENGTHS OF LAP SPLICES ANCHORED BY HIGH-STRENGTH HEADED BARS

S. C. CHUN[*] AND J. G. LEE[†]

[*] Department of Architectural Engineering, Mokpo National University
Dorim-ri, Cheonggye-myeon, Muan-gun, Jeonnam, 534-729, Korea
e-mail: scchun @mokpo.ac.kr

[†] Department of Architectural Engineering, Mokpo National University
Dorim-ri, Cheonggye-myeon, Muan-gun, Jeonnam, 534-729, Korea
e-mail: carrot3737@nate.com

Key words: Headed bar, Anchorage, Lap splice, Bond, Bearing

Abstract: Design specifications for headed bars were recently amended in ACI 318 and KCI 2012. These specifications have limitations on bar strength, bar diameters, concrete strength, and so on, due to lack of test data. Experiments of lap splices with high-strength headed bars were conducted to investigate the anchorage behavior of high-strength headed reinforcement. Headed bars of Grade 600 MPa were used and main variables include splice length, spacing between bars, bar diameter, concrete strength, and confinement. Observations of cracking behavior, strain measurements of reinforcement, and strength are reported. The strengths of lap splices with Grade 600 MPa are compared with design codes and previous models. The behavior of unconfined laps is compared to the behavior of confined laps. Test results show that the current codes do not provide a conservative design for high-strength headed bars and transverse reinforcement is more important than cover thickness to confine splice laps.

1 INTRODUCTION

Headed bars as shown in Figure 1 provide an alternative to hooked bars and assist in alleviating steel congestion, especially in exterior beam-column joints where multiple structural members join. In ACI 318-08 [1], the development of headed bars was first introduced. However, because the design equations of ACI 318 were based on limited test data [2-4], the restrictions on strengths and bar details were strict. Specified design yield strength of headed bars shall not exceed 420 MPa for headed bars but reinforcing bars with yield strength of higher than 420 MPa are allowed as longitudinal reinforcement in many design codes including Eurocode [5], ACI [6] and KCI [7]. Therefore, new provisions for high-strength headed bars are required. In this study, lap splice specimens with high-strength headed bars were tested to investigate the anchorage behavior of high-strength headed reinforcement.

Figure 1: Headed bars.

2 EXPERIMENTAL PROGRAM

2.1 Specimen variables

A typical lap splice specimen is shown in Figure **2**. Two reinforcing bars were lapped at the midpoint of the specimen. Nine specimens were unconfined within the lap zone, without stirrups or other supplementary reinforcement used to enhance the performance of the splice as shown in Figure 2(b). Three confined specimens with transverse reinforcement were also tests. The configuration used in these test specimens was chosen since it may give a conservative, i.e. low, strength.

Specimen variables include splice length L_s, bar spacing/cover c, transverse reinforcement contents K_{tr}, bar diameter d_b, and concrete compressive strength f_c' . Details of all specimens are listed in Table 1.

The lap splice length varied from $15d_b$ to $25d_b$. This range of splice lengths were chosen to ensure that the lap splices would fail before the longitudinal tension steel could yield.

Two kinds of c values were tested: one is $2d_b$ which is in accordance with clause 12.6 of the ACI 318-11 [6] and the other is $1d_b$ to accommodate the smaller spacing or cover which simulate a more practical and actual spacing. Splitting cracks were anticipated to form through the side cover and between the bars and the bottom covers were designed to be larger than the side cover or half of the clear spacing between bars.

Two confinement details were tested: one using stirrups placed along entire splice length (a fully confined splice) and the other with stirrups placed at the ends of the lap zone (a locally confined splice) as shown in Figure 2(c).

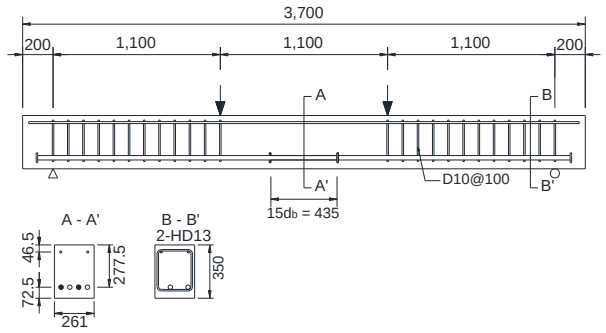

(a) Details of specimen

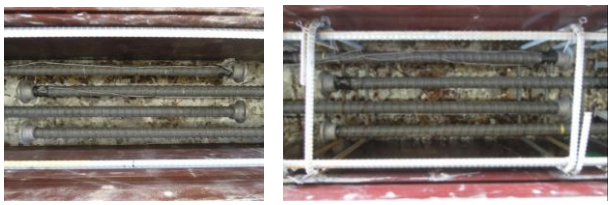

(b) Unconfined specimen (c) Locally confined specimen

Figure 2: Lap splices by headed bars.

Table 1: Test matrix

Specimens	$B\times H\times L$ [mm]	d_b [mm]	f_c' [MPa]	L_s/d_b	c/d_b	K_{tr}/d_b
D29-S2-F42-L15	261×350×3700	29	42	15	1	-
D29-S2-F42-L20				20	1	-
D29-S2-F42-L25				25	1	-
D29-S4-F42-L15	408×350×3700			15	2	-
D29-S4-F42-L20				20	2	-
D25-S2-F42-L20	225×350×3700	25		20	1	-
D25-S2-F42-L25				25	1	-
D29-S2-F21-L20	261×450×4500	29	21	20	1	-
D29-S2-F21-L25				25	1	-
D29-S2-F42-L15-Con.	261×350×3700		42	15	1	0.76
D29-S2-F42-L20-Con.				20	1	0.76
D29-S2-F42-L20-LCon.				20	1	0.34

* Notations: B, H, and L are width, height, and length of specimen, respectively; c is the smaller of the minimum concrete cover or 1/2 of the clear spacing between bars; K_{tr} is transverse reinforcement index (= $(40A_{tr})/(s_{tr}n)$, refer to clause 12.2 of ACI 318-11).

In addition, two bar diameters, 25 mm and 29 mm were chosen to examine the effect of bar size. Two kinds of concrete compressive strength, 21 MPa and 42 MPa were used.

2.2 Specimen design

All spliced bars were cast as bottom bars. Dimensions of the specimens were selected to ensure a flexural behavior until splitting failure. The beam cross section and length were summarized in Table 1.

2.3 Test setup and Instrumentation

The specimens were tested utilizing four-point loading test schematics as shown in Figure 3. Universal Test Machine (UTM) with a capacity of 3000 kN was used to apply a monotonic load.

Instrumentation of the specimens consisted of load-beam deflection measurements and strain measurements along the bars. To determine the head bearing and bond contributions, electrical resistance strain gages were attached to two points on two bars. The gages were mounted at a distance of $1d_b$ from a head face and out of the splice length but within the constant moment region.

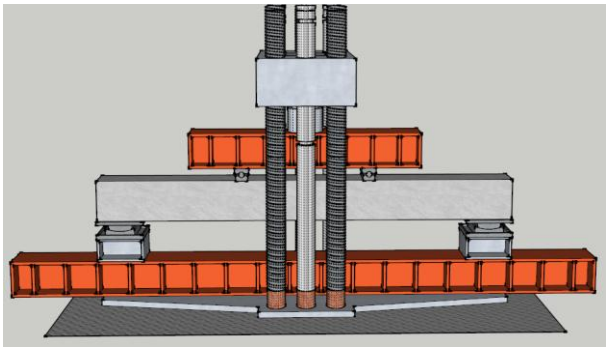

Figure 3: Test setup.

3 TEST RESULTS

3.1 Overall behavior and failure modes

First cracking in the specimens usually consisted of transverse flexural cracks within the constant moment zone. Especially, cracks at the ends of the splice length were dominant. Near failure, one or more longitudinal cracks would form over the splice lengths. All of the specimens failed in a brittle and sudden manner. Failure occurred with a rapid loss of capacity.

In unconfined specimens, longitudinal cracks were obviously observed and bottom cover concrete spalled in many unconfined specimens as shown in Figure 4(a). In confined specimens, the longitudinal cracks were not apparent compared with transverse flexural cracks as shown in Figure 4(c). In locally confined specimen, the longitudinal cracks were clear but not as much as unconfined specimens as shown in Figure 4(b).

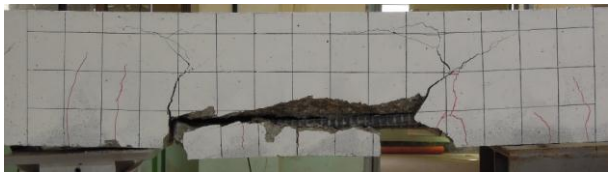

(a) Unconfined specimen

(b) Locally confined specimen

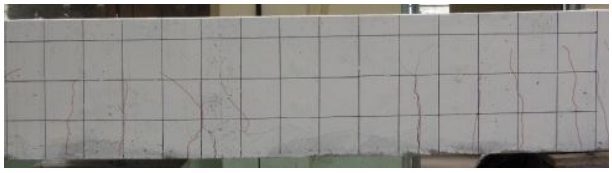

(c) Confined specimen

Figure 4: Typical specimen failures of S2F42L20-series.

3.2 Bar stresses

Failure loads P_e of the specimens and concrete compressive strengths at test date were summarized in Table 2. The anchorage strengths $f_{s,e}$, i.e. developed stresses at the time of failure, were obtained based on moment-curvature calculations with Collins and Mitchell model [8] of concrete stress-strain relationship and were shown in Table 2. As

splice length, transverse reinforcement index, and concrete compressive strength increase, the bar stresses increase. However, the c value did not much affect the bar stresses; the bar stresses of the specimens with $c = 2d_b$ were enhanced by only 5% compared with the specimens with $c = 1d_b$. There is no significant difference between specimens with bar diameters of 25 mm and 29 mm.

The developed bar stresses were compared with predictions by ACI 318-11 [6] and Thompson et al. [9], in Figure 5 and Table 2. The average ratios of developed to calculated values for unconfined specimens are only 0.54 and 0.42 by ACI 318 and Thompson et al, respectively. For confined specimens, the average ratios increase somewhat, 0.85 and 0.66 by ACI 318 and Thompson et al, respectively. It means that the current design provisions cannot give a conservative result for high-strength reinforcing bars and, especially, the headed bars without transverse reinforcement cannot be effectively developed.

The bar stress consists of bond and head bearing contributions. To investigate the development of bar stresses, the contributions of bond and bearing on the bar stress were examined in following sections.

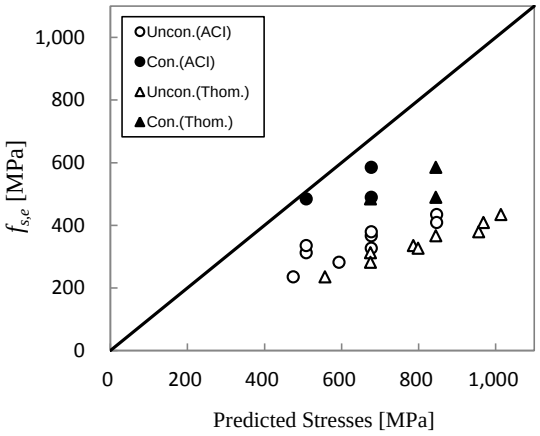

Figure 5: Comparisons of bar stresses with predicted stresses

3.3 Stresses developed by head bearing

The bar stresses developed by head bearing $f_{brg,e}$ were determined from the measured strains at a distance of $1d_b$ from a head face and summarized in Table 2. Figure 6 shows the stresses developed by head bearing with varying splice lengths for unconfined specimens where the stresses were normalized with $\sqrt{f_c'}$ to eliminate the difference of concrete compressive strengths. It shows that the stresses developed by head bearing are not related to splice length. In addition, there is no

Table 2: Test results

Specimens	f_c' [MPa]	P_e [kN]	$f_{s,e}$ [MPa]	$f_{s,\mathrm{ACI}}$ [MPa]	$f_{s,T}$ [MPa]	$f_{brg,e}$ [MPa]	$f_{b,e}$ [MPa]	$f_{b,O}$ [MPa]	$f_{b,408}$ [MPa]
D29-S2-F42-L15	41.4	88	312	508	675	48	264	242	274
D29-S2-F42-L20		104	367	677	845	52	314	287	313
D29-S2-F42-L25		122	434	847	1014	58	376	332	351
D29-S4-F42-L15		97	335	508	787	58	277	339	319
D29-S4-F42-L20		110	379	677	956	57	322	416	376
D25-S2-F42-L20		76	326	677	799	47	280	287	313
D25-S2-F42-L25		95	408	847	968	49	359	332	351
D29-S2-F21-L20	20.3	76	235	475	557	37	198	201	262
D29-S2-F21-L25		91	282	593	676	38	244	233	294
D29-S2-F42-L15-Con.	41.4	136	484	508	675	133	352	315	338
D29-S2-F42-L20-Con.		163	585	677	845	140	445	384	395
D29-S2-F42-L20-LCon.		138	489	677	845	86	403	331	353

* Notations: P_e is a measured peak load; $f_{s,e}$ is a measured anchorage strength at P_e; $f_{s,\mathrm{ACI}}$ is a predicted anchorage strength by clause 12.6 of ACI 318-11; $f_{s,T}$ is a predicted anchorage strength by Thompson et al. [9]; $f_{brg,e}$ is a measured stress developed by end bearing; $f_{b,e}$ is a measured stress developed by bond.

significant difference with different bar diameter and *c* value.

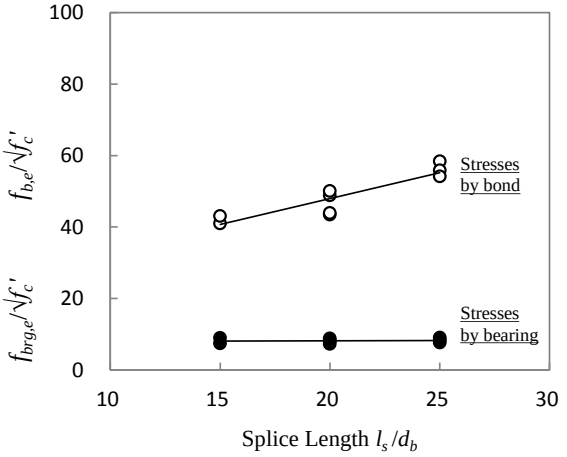

Figure 6: Stresses developd by bond and bearing for unconfined specimens.

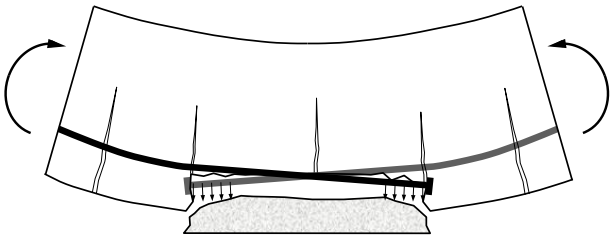

Figure 7: Cover spalling in lap zone due to prying action caused by beam curvature [10].

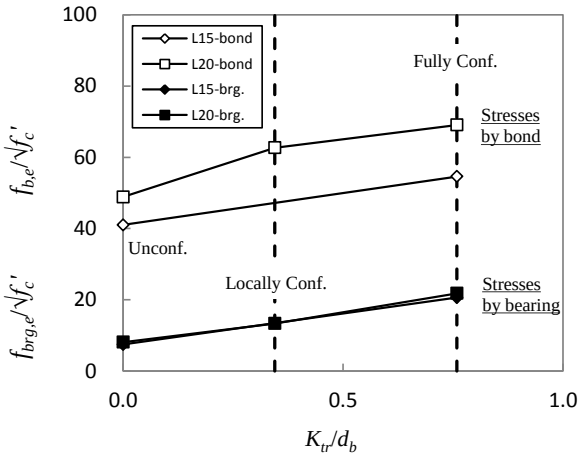

Figure 8: Stresses developd by bond and bearing for confined specimens.

The mean value is only $8.2\sqrt{f_c'}$ MPa and it is significantly low compared with test results of Thompson et al. [4] and end bearing contributions in compression lap splices [11]. These low bearing contributions represents that the unconfined splices failed before the end bearing were activated. Because of the absence of transverse reinforcement, *prying action* as shown in Figure 7 could not be prevented and the unconfined splices failed prematurely.

For the confined specimens, the end bearing contributions increased dramatically as shown in Figure 8. Providing two stirrups at each end, the bearing contributions increased by 65%, i.e. from 52 MPa to 86 MPa. For the fully confined splices where transverse reinforcement was placed along splice length, the end bearing contributions increased by 73% on average.

3.4 Stresses developed by bond

The bar stresses developed by bond $f_{b,e}$ were obtained by deducting the stresses developed by the end bearing from the bar stresses and summarized in Table 2. Figure 6 shows the stresses developed by bond with varying splice lengths for unconfined specimens where the stresses were normalized with $\sqrt{f_c'}$. It shows that the stresses developed by bond are almost linearly proportional to the splice lengths.

The stresses developed by the bond for unconfined splices are compared with the values $f_{b,calc}$ predicted using well-known expressions for the bond strengths of tension splices (Eq. (1) [12] and (2) [13]) in Figure 9. The stresses developed by the bond are almost same to the predicted values by Eq. (1) but are less than the predicted values by Eq. (2). Since the expression of ACI Committee 408 is an advanced one based on a large database, it is found that the bond strengths of the headed bars are not fully developed in unconfined splices. Similarly to the stresses developed by end bearing, the bond strengths in unconfined splices could not be developed completely due to *prying action.*

$$f_{b,O} = \left[\left(0.4 + \frac{c}{d_b}\right)\frac{l_s}{d_b} + 16.6\right]\sqrt{f_c'} \qquad (1)$$

$$f_{b,408} = \left[1.82\frac{l_s}{d_b}\left(\frac{c_{\min}}{d_b}+0.5\right)+57.4\right] \times\left(0.1\frac{c_{\max}}{c_{\min}}+0.9\right) f_c'^{1/4} \quad (2)$$

where $c_{\min}$ = min (c_c, c_s), $c_{\max}$ = max (c_c, c_s), c_c is the minimum concrete cover, c_s = min (c_{so}, c_{si} + 6.35 mm (0.25 in.)), c_{so} is the side cover for a reinforcing bar, c_{si} is 1/2 of the bar clear spacing, and $(0.1c_{max}/c_{min}+0.9) \leq 1.25$.

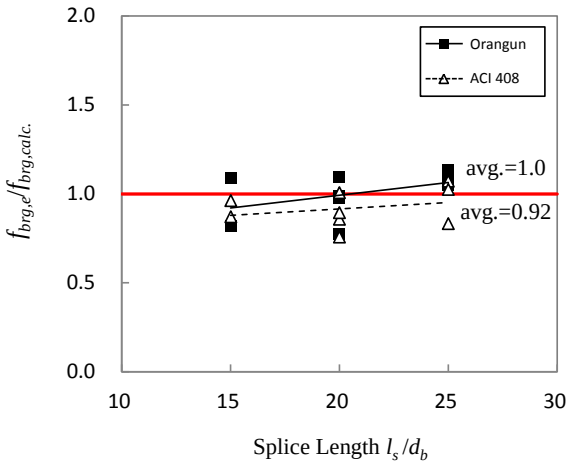

Figure 9: Comparisons of stresses developed by bond with predicted stresses for unconfined splices

For the confined specimens, the stresses developed by bond increased significantly as shown in Figure 8 and Table 2. The locally confined splice also had a lot higher bond strength than the unconfined splice even though only two stirrups were placed at ends of the splice length. The bond strength of the locally confined splice is higher over 10% than the predicted values by Eq. (1) and (2). This means that if *prying action* is prevented, the bond strengths can be fully developed. By placing stirrups along the splice length, the stresses developed by bond were enhanced by 37% as shown in Figure 8.

4 CONCLUSIONS

Splice tests were carried out to assess the anchorage strength of high-strength headed bars. Twelve beams reinforced with lap-spliced headed bars were tested. The following conclusions can be drawn based on the results of the tests.

1. The current design provisions do not give a conservative result for high-strength reinforcing bars, especially, without transverse reinforcement.
2. Without transverse reinforcement, the head bearing cannot be activated due to *prying action*. By placing transverse reinforcement at ends of splice length, the end bearing contributions increased dramatically. For the fully confined splices where transverse reinforcement was placed along splice length, the end bearing contributions increased by 73% on average.
3. The bond strengths in unconfined splices were not developed completely due to *prying action*. However, if transverse reinforcement is provided, the bond strengths can be developed more than the bond strength of a straight bar.

ACKNOWLEMENT

This research was supported by Basic Science Re-search Program through the National Research Foundation of Korea (NRF) funded by the Ministry of Education, Science and Technology (No. 2011-0013828). The authors wish to thank Boo Won B.M.S. Co. Ltd., Korea for providing the headed bars used in the tests.

REFERENCES

[1] ACI Committee 318, 2008. *Building Code Requirements for Structural Concrete (ACI 318-08) and Commentary*, American Concrete Institute, p. 465.

[2] Thompson, M.K., Ziehl, M.J., Jirsa, J.O., and Breen, J. E., 2005, CCT Nodes Anchored by Headed Bars-Part 1: Behavior of Nodes. *ACI Structural Journal*, 102(6): 808-815.

[3] Thompson, M.K., Jirsa, J.O. and Breen, J.E., 2006. CCT Nodes Anchored by Headed Bars-Part 2: Capacity of Nodes. *ACI Structural Journal*, 103(1): 65-73.

[4] Thompson, M.K., Ledesma, Antonio, Jirsa,

J.O., and Breen, J.E., 2006. Lap Splices Anchored by Headed Bars. *ACI Structural Journal*, 103(2): 271-279.

[5] Comité Euro-International du Béton, 2012. *CEB-FIP Model Code 2010* Final draft - Volume 1.

[6] ACI Committee 318, 2011. *Building Code Requirements for Structural Concrete (ACI 318-11) and Commentary*, American Concrete Institute, p. 503.

[7] Korea Concrete Institute, 2012. *Concrete Structure Design Code*, Kimoondang.

[8] Collins, M.P. and D. Mitchell, 1991. *Prestressed Concrete Structures*. Prentice Hall College Div.

[9] Thompson, M.K., Jirsa, J.O., and Breen, J.E., 2006. Behavior and Capacity of Headed Reinforcement. *ACI Structural Journal*, 103(4): 522-530.

[10] Chun, S.-C., Lee, S.-H., and Oh, B., 2010. Compression Lap Splice in Unconfined Concrete of 40 and 60 MPa (5800 and 8700 psi) Compressive Strengths. *ACI Structural Journal*, 107(2): 170-178.

[11] Thompson, M.K., 2002. The Anchorage Behavior of Headed Reinforcement in CCT Nodes and Lap Splices. The University of Texas at Austin: Austin. p. 502.

[12] Orangun, C.O., Jirsa, J.O., and Breen, J.E., 1977. A Reevaluation of Test Data on Development Length and Splices. *ACI Journal*, 74(3): 114-122.

[13] ACI Committee 408, 2003. Bond and Development of Straight Reinforcing Bars in Tension (ACI 408R-03). American Concrete Institute: p. 49.